

Extracting the condensate density from projection experiments with Fermi gases

A. Perali, P. Pieri, and G.C. Strinati

Dipartimento di Fisica Università di Camerino, I-62032 Camerino, Italy

(Dated: November 1, 2019)

A debated issue in the physics of the BCS-BEC crossover with trapped Fermi atoms is to identify characteristic properties of the superfluid phase. Recently, a condensate fraction was measured on the BCS side of the crossover by sweeping the system in a fast (nonadiabatic) way from the BCS to the BEC sides, thus “projecting” the initial many-body state onto a molecular condensate. We analyze here the theoretical implications of these projection experiments, by identifying operatively the measured quantities and relating them to the many-body correlations occurring in the BCS-BEC crossover. Calculations are presented over wide temperature and coupling ranges, by including pairing fluctuations on top of mean field. A prediction is made for a reduced molecular fraction, and the role of Pauli blocking on extracting the condensate fraction is addressed.

PACS numbers: 03.75.Hh,03.75.Ss

The current experimental advances with trapped Fermi atoms have attracted much interest in the physics of the BCS-BEC crossover. In this context, one of the most debated issues is the unambiguous detection of superfluid properties on the BCS side of the crossover. Several attempts have been made in this direction. They include absorption images of the “projected” density profiles for ^{40}K [1] and ^{6}Li [2], rf spectroscopy to detect single-particle excitations [3], and measurements of collective modes [4, 5].

In particular, the experimental procedure of Refs. [1, 2] pairwise “projects” fermionic atoms onto molecules, by preparing the system of trapped Fermi atoms on the BCS side with a tunable Fano-Feshbach resonance and then rapidly sweeping the magnetic field to the BEC side. In this way, the same two-component fit of density profiles routinely used for Bose gases is exploited to extract from these “projected” density profiles the analog of a condensate fraction, which is now associated with the equilibrium state on the BCS side before the sweep took place.

Purpose of this paper is to provide a theoretical interpretation of the experiments of Refs. [1, 2], by obtaining the “projected” density profiles in terms of the correlation functions of the Fermi gas at equilibrium. This will be based on a number of physical assumptions which we associate with the experimental procedure of Refs. [1, 2]. Our calculation evidences how the projection procedure amplifies the emergence of the condensate as the temperature is lowered below T_c , when compared with the ordinary density profiles of Ref. [6]. We also attempt an analysis of the “projected” density profiles in terms of a two-component fit, in analogy to what is done with the experimental data [1, 2]. The role played by Pauli blocking in leading to an overestimate of the condensate fraction extracted from these fits is pointed out. A prediction is further made of a reduced molecular fraction that depends on the initial many-body state, in agreement with a late experimental evidence [7].

Inclusion of pairing fluctuations on top of mean field

along the lines of Ref. [8] enables us to cover a wide temperature range even in the intermediate- and strong-coupling regimes, in contrast to Refs. [9, 10] where only mean field was taken into account.

To describe the “projected” density profiles of Refs. [1, 2], we consider the boson-like field operator:

$$\Psi_B(\mathbf{r}) = \int d\rho \phi(\rho) \psi_\downarrow(\mathbf{r} - \rho/2) \psi_\uparrow(\mathbf{r} + \rho/2). \quad (1)$$

Here, $\psi_\sigma(\mathbf{r})$ is a fermion field operator with spin σ , and $\phi(\rho)$ a real and normalized function which specifies the probability amplitude for the fermion pair. An operator of the form (1) was considered in Ref. [11] to obtain the condensate density for composite bosons.

Our theoretical analysis of the experiments of Refs. [1, 2] is based on the following *physical assumptions*, that we infer from the experimental procedure:

- (i) Atoms of a specific spin state were detected, which originated from the dissociation of molecules after applying an rf pulse. The object of the measurement is thus the bosonic (molecular) density $n_B(\mathbf{r})$ at position \mathbf{r} in the trap (and not the fermionic (atomic) density $n(\mathbf{r})$).
- (ii) When rapidly sweeping the magnetic field, the internal wave function of a molecule should follow the field to some extent. There are reasons to believe [12] that the molecules actually form on the BEC side, not too far from the unitarity limit. We assume correspondingly that the wave function in the expression (1) refers to some “final” coupling value on the BEC side, and represent it accordingly by $\phi_f(\rho)$. In analogy with the original Cooper argument [13], we then identify ϕ_f with the bound-state solution of the two-body problem with the condition that its Fourier transform $\phi_f(\mathbf{k})$ vanishes when the magnitude of the wave vector \mathbf{k} is smaller than the characteristic value $k_{\mu_f} = \sqrt{2m\mu_f}$ for $\mu_f > 0$ (m being the fermion mass), while no constraint is enforced for $\mu_f < 0$. Here, the value of the chemical potential μ_f depends on the “final” coupling at which the molecular state is assumed to form. Lacking precise information

about this coupling, we shall present our calculations for two coupling values which we consider representative of the cases when μ_f is positive or negative, being still not too far from the unitarity limit.

(iii) In the experiments, bosonic Thomas-Fermi (TF) profiles for the molecular condensate were extracted from position-dependent density profiles, thus entailing an assumption of thermal equilibrium. We assume that this thermal equilibrium corresponds to the state prepared *before* the rapid sweep of the magnetic field. The validity of this assumption has been lately supported by an experimental study of the formation time of a fermion-pair condensate [7]. Thermal averages used in the calculations are then interpreted as $\langle \dots \rangle_i$ where the suffix i stands for “initial”.

All these assumptions are summarized by stating that the “*projected*” bosonic density profile given by

$$n_B^{fi}(\mathbf{r}) = \langle \Psi_B^f(\mathbf{r})^\dagger \Psi_B^f(\mathbf{r}) \rangle_i \quad (2)$$

represents what is actually measured in the experiments of Refs. [1, 2]. In this expression, the boson-like field operator of Eq. (1) contains the *final* molecular wave function $\phi_f(\rho)$ on the BEC side of the crossover, while the thermal average $\langle \dots \rangle_i$ is taken with reference to the state in which the system was *initially* prepared.

Consistently with our previous work [14], we describe the interaction term of the many-fermion Hamiltonian via an effective single-channel model. The parameter $(k_F a_F)^{-1}$ then drives the crossover from the BCS side (identified by $(k_F a_F)^{-1} \lesssim -1$) to the BEC side (identified by $1 \lesssim (k_F a_F)^{-1}$) across the unitarity limit $(k_F a_F)^{-1} = 0$. Here, a_F is the two-fermion scattering length and the Fermi wave vector k_F results by setting $k_F^2/(2m)$ equal to the noninteracting Fermi energy.

The calculation proceeds by expressing the four-fermion field operator in Eq. (2) in terms of the two-particle Green’s function $\mathcal{G}_2(1, 2, 1', 2') = \langle T_\tau [\Psi(1) \Psi(2) \Psi^\dagger(2') \Psi^\dagger(1')] \rangle$, where T_τ is the imaginary-time ordering operator. We have introduced the Nambu representation $(\Psi_1(\mathbf{r}) = \psi_\uparrow(\mathbf{r}), \Psi_2(\mathbf{r}) = \psi_\downarrow^\dagger(\mathbf{r}))$ as well as the notation $1 = (\mathbf{r}_1, \tau_1, \ell_1)$ with imaginary time τ and Nambu component ℓ . The thermal average contains the grand-canonical Hamiltonian $K = H - \mu N$ with fermionic chemical potential μ (the suffix i being understood as specified above), and $\Psi(1) = \exp\{K\tau_1\} \Psi_{\ell_1}(\mathbf{r}_1) \exp\{-K\tau_1\}$.

The two-particle Green’s function \mathcal{G}_2 is, in turn, expressed in terms of the many-particle T-matrix, by solving formally the Bethe-Salpeter equation as follows:

$$\begin{aligned} \mathcal{G}_2(1, 2, 1', 2') &= \mathcal{G}(1, 1') \mathcal{G}(2, 2') - \mathcal{G}(1, 2') \mathcal{G}(2, 1') \\ &- \int d3456 \mathcal{G}(1, 3) \mathcal{G}(6, 1') T(3, 5; 6, 4) \mathcal{G}(4, 2') \mathcal{G}(2, 5) \end{aligned} \quad (3)$$

where $\mathcal{G}(1, 1') = -\langle T_\tau [\Psi(1) \Psi^\dagger(1')] \rangle$ is the fermionic single-particle Green’s function. Accordingly, the “*projected*” bosonic density (2) reads:

$$n_B^{fi}(\mathbf{r}) = \int d\boldsymbol{\rho} d\boldsymbol{\rho}' \phi_f(\rho) \phi_f(\rho') \mathcal{G}_2^i(1, 2, 1', 2') \quad (4)$$

where $1 = (\mathbf{r} - \rho/2, \tau + 2\eta, \ell = 2)$, $2 = (\mathbf{r} + \rho'/2, \tau, \ell = 1)$, $1' = (\mathbf{r} + \rho/2, \tau + 3\eta, \ell = 1)$, and $2' = (\mathbf{r} - \rho'/2, \tau + \eta, \ell = 2)$ (η being a positive infinitesimal).

Implementation of the above expressions to the trapped case is readily obtained via a local-density approximation, whereby a local gap parameter $\Delta(\mathbf{r})$ is introduced and the chemical potential μ is replaced (whenever it occurs for both “initial” and “final” couplings) by the quantity $\mu(\mathbf{r}) = \mu - V(\mathbf{r})$ that accounts for the trapping potential $V(\mathbf{r})$.

The three terms on the right-hand side of Eq. (3) correspond to physically different contributions to the expression (4). In particular, the first term can be written as $|\alpha_{fi}|^2$, where $\alpha_{fi} = \int d\boldsymbol{\rho} \phi_f(\rho) \mathcal{G}_{12}^{(i)}(\rho, \tau = -\eta)$ represents the *overlap* between the fermionic correlations (which are embodied in the anomalous single-particle Green’s function $\mathcal{G}_{12}^{(i)}$) and the molecular wave function ϕ_f . This contribution vanishes with the gap parameter Δ when approaching T_c , and is identified with the *condensate density* for composite bosons when both the “initial” thermal equilibrium and the “final” molecular wave function are taken at the same coupling deep in the BEC side of the crossover [11]. Only this contribution was considered in Ref. [10] in connection with the experiments of Refs. [1, 2].

The second term on the right-hand side of Eq. (3) represents fermionic correlations in the normal state, which are relevant in the presence of an underlying Fermi surface. This term is most sensitive to the “final” molecular wave function ϕ_f being affected by Pauli blocking when μ_f is positive. This term would be irrelevant when both the “initial” thermal equilibrium and the “final” molecular wave function were taken deep in the BEC side. When μ_f is positive, this term can lead to an overestimate of the value of the condensate fraction when the “projected” density profiles are fitted in terms of TF and Gaussian functions, as shown below. Both this and the previous contribution were considered in Ref. [9] (where the “final” coupling was, however, taken deep in the BEC region).

The third term on the right-hand side of Eq. (3) will be calculated in the following within the off-diagonal BCS-RPA approximation considered in Ref. [11]. This contribution is identified with the *noncondensate density* for composite bosons when both the “initial” thermal equilibrium and the “final” molecular wave function are taken at the same coupling deep in the BEC side [11]. It is thus of particular importance for increasing temperature when approaching the normal phase.

We have verified that, when $i = f$ deep in the BEC region, the “*projected*” density profile $n_B^{ii}(\mathbf{r})$ coincides with (half) the ordinary density profile $n(\mathbf{r})$ calculated

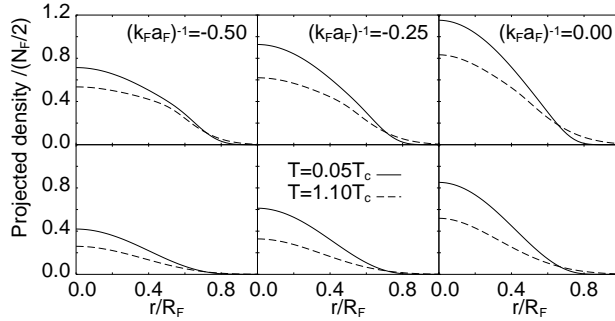


FIG. 1: Axially-integrated “projected” density profiles for three “initial” coupling values and for two “final” couplings: 0.40 (upper panel) and 1.50 (lower panel). The radial distance r is in units of the fermionic Thomas-Fermi radius R_F .

at the same coupling. In this and the following calculations, the values for the local chemical potential and gap parameter, to be inserted in the expression (4) for $n_B^{fi}(\mathbf{r})$, are taken from Ref. [6] where pairing fluctuations are included on top of mean field. When $i \neq f$ (as realized by the experiments of Refs. [1, 2]), the above three contributions taken together determine the “projected” density profiles $n_B^{fi}(\mathbf{r})$, to be confronted with the ones measured experimentally.

Figure 1 shows the axially-integrated “projected” density profiles calculated for the coupling values $(k_F a_F)_i^{-1} = (-0.50, -0.25, 0.00)$ and for the two representative values 0.40 (upper panel) and 1.50 (lower panel) of the “final” coupling $(k_F a_F)_f^{-1}$. Two characteristic temperatures (just above the critical temperature and near zero temperature) are considered in each case. Note the marked temperature dependence of the “projected” density profiles when entering the superfluid phase, as signaled by the emergence of a “condensate” component near the center of the trap. This contrasts the milder dependence (especially on the BCS side) of the density profiles without projection, as reported in Ref. [6]. The “projection” technique introduced in Ref. [1] is thus demonstrated to *amplify* the effects due to the presence of a condensate on the density profiles, which would otherwise be almost temperature independent on the BCS side of the crossover.

In Fig. 1 the densities are normalized to half the total number N_F of fermionic atoms. This number differs, in general, from the total number N_{mol} of molecules obtained by integrating the “projected” density profiles. In particular, N_{mol} can vary significantly when scanning the “initial” value of $(k_F a_F)^{-1}$ on the BCS side of the crossover for given “final” molecular-like state. This effect is shown in Fig. 2 for the same temperatures and “final” couplings of Fig. 1. Our finding that the total number N_{mol} of molecules constitutes only a fraction of the original atom number $N_F/2$ for each spin state is supported by the experimental results of Refs. [1] and [2], which report values up to 60% – 80% and 90%, in

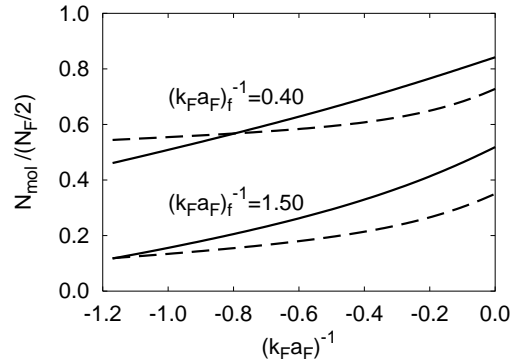


FIG. 2: Ratio $N_{mol}/(N_F/2)$ vs $(k_F a_F)^{-1}$ on the BCS side of the crossover, for the same temperatures and “final” couplings of Fig. 1.

the order. In addition, our prediction that the reduced value of the molecular fraction depends on the “initial” many-body state is in agreement with the experimental evidence recently reported in Ref. [7].

In our procedure, the “condensate” and “noncondensate” components of the “projected” density profiles are calculated separately. By our definition, they correspond to the first term and to the remaining terms on the right-hand side of Eq. (3), respectively. The *condensate fraction* is obtained accordingly from the ratio of the corresponding areas. Yet, the total “projected” density profiles obtained theoretically could be analyzed in terms of a two-component fit with a TF plus a Gaussian function (or, better, a $g_{3/2}$ function for the Bose gas), in analogy to what is done to analyze the experimental data [1, 2]. This kind of analysis is reported in Fig. 3 for the two low-temperature curves shown in the right panels of Fig. 1. In both cases, a quite good overall fit is obtained by the χ^2 -square method (with small deviations only at large radial distances). This figure compares the TF component of the fit (dashed line) with the theoretical “condensate” component as defined above (full line), and the $g_{3/2}$ component of the fit (dotted line) with the theoretical “noncondensate” component (dashed-dotted line). The separate comparisons agree rather well for the value 1.50 of the “final” coupling (right panel), while discrepancies occur for the value 0.40 (left panel). These discrepancies stem from the presence of the second term on the right-hand side of Eq. (3), which contributes mostly to the TF component of the fit owing to the peculiar shape of the corresponding “projected” density profile. As a consequence, the value 0.76 of the (apparent) condensate fraction extracted from the fit at the unitarity limit when the “final” coupling equals 0.40 exceeds by more than 50% the corresponding theoretical value 0.49 (when the “final” coupling equals 1.50, on the other hand, the difference is only about 1%). This result indicates that Pauli blocking (by affecting the molecular-like wave function) can lead to an overestimate of the value of the condensate fraction as extracted from the fits. This effect could

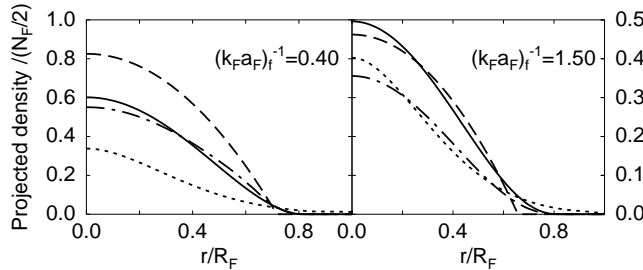


FIG. 3: Two-component (TF plus $g_{3/2}$) fit of the “projected” density profiles at the unitarity limit for $T/T_c = 0.05$. The meaning of the different curves is explained in the text.

thus have contributed to the rather large values of the condensate fraction extracted from the data of Ref. [2]. By the same token, Fig. 3 shows that this effect is absent when the “final” coupling is taken at the value 1.50 where Pauli blocking is no longer effective.

Extention of this analysis to “initial” couplings on the BCS side evidences unconventional functional forms of the theoretical condensed and noncondensed contributions to the “projected” density profiles, so that enforcement of the above two-component fit is bound to fail. For this reason, we prefer to get the condensed and noncondensed contributions directly from our theoretical expressions, without performing such a two-component fit.

In Fig. 4 the condensate fraction N_0/N_{mol} (obtained from our theoretical expressions) is plotted vs $(k_F a_F)^{-1}$ on the BCS side of the crossover. The lowest temperature $T/T_c = 0.05$ and two “final” couplings 0.40 (full line) and 1.50 (broken line) are considered. The analogous quantities extracted from the experiments of Ref. [1] (dots) and of Ref. [2] (squares) are also reported. The agreement between the overall trends of the theoretical and experimental curves appears satisfactory, although quantitative discrepancies result between the two sets of curves. They might be due to an overestimate of the TF component of the fits in Ref. [2] for the reasons discussed above, and to a possible underestimate of the condensate component in Ref. [1] due to a preferential loss of molecules in the condensate itself. As a further comparison with the experimental data, we have also verified that the linear dependence between $N_{mol}/(N_F/2)$ and N_0/N_{mol} reported in Fig. 4(b) of Ref. [2] is reproduced by our calculation (albeit with a larger slope) for the value 0.40 of the “final” coupling, while a slight upturn of the curve results for the value 1.50 (see the inset of Fig. 4).

Our theoretical “projected” density profiles are calculated when molecules form on the BEC side near the unitarity limit. We expect, in fact, that the further ramp of the magnetic field and the subsequent expansion of the cloud performed in the experiments should have no influence on the values of N_{mol} and N_0/N_{mol} .

In conclusion, the present theoretical approach, by as-

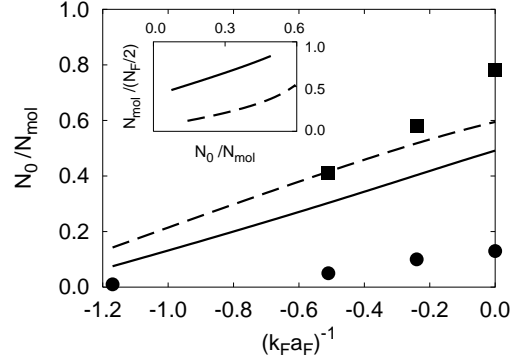


FIG. 4: Condensate fraction N_0/N_{mol} vs $(k_F a_F)^{-1}$ on the BCS side of the crossover at low temperature for two different “final” couplings (see text). The inset reports $N_{mol}/(N_F/2)$ vs N_0/N_{mol} for the same couplings.

sociating a suitable quantum-mechanical operator to the “projection” procedure of Refs. [1, 2], has enabled us to operatively define a fermionic pair condensate even on the BCS side of the crossover, thus confirming that the experiments of Refs. [1, 2] detect a property of the superfluid phase.

We are indebted to C. Salomon and H. Stoof for discussions, and to D. Jin for a critical reading of the manuscript. This work was partially supported by the Italian MIUR with contract Cofin-2003 “Complex Systems and Many-Body Problems”.

- [1] C.A. Regal, M. Greiner, and D.S. Jin, Phys. Rev. Lett. **92**, 040403 (2004).
- [2] M.W. Zwierlein, C.A. Stan, C.H. Schunck, S.M.F. Raupach, A.J. Kerman, and W. Ketterle, Phys. Rev. Lett. **92**, 120403 (2004).
- [3] C. Chin, M. Bartenstein, A. Altmeyer, S. Riedl, S. Jochim, J.H. Denschlag, and R. Grimm, Science **305**, 1128 (2004).
- [4] J. Kinast, S.L. Hemmer, M.E. Gehm, A. Turlapov, and J.E. Thomas, Phys. Rev. Lett. **92**, 150402 (2004).
- [5] M. Bartenstein, A. Altmeyer, S. Riedl, S. Jochim, C. Chin, J.H. Denschlag, and R. Grimm, Phys. Rev. Lett. **92**, 203201 (2004).
- [6] A. Perali, P. Pieri, L. Pisani, and G.C. Strinati, Phys. Rev. Lett. **92**, 220404 (2004); A. Perali, P. Pieri, and G.C. Strinati, Phys. Rev. Lett. **93**, 100404 (2004).
- [7] M.W. Zwierlein, C.H. Schunck, C.A. Stan, S.M.F. Raupach, and W. Ketterle, cond-mat/0412675.
- [8] P. Pieri, L. Pisani, and G.C. Strinati, Phys. Rev. B **70**, 094508 (2004).
- [9] R.B. Diener and T.L. Ho, cond-mat/0404517.
- [10] A.V. Avdeenkov and J.L. Bohn, cond-mat/0404653.
- [11] N. Andrenacci, P. Pieri, and G.C. Strinati, Phys. Rev. B **68**, 144507 (2003).
- [12] C. Salomon, private communication.
- [13] L.N. Cooper, Phys. Rev. **104**, 1189 (1956).
- [14] S. Simonucci, P. Pieri, and G.C. Strinati, cond-mat/0407600 (to appear in Europhys. Lett.).